Electron Temperature Measurement Using Electron Bernstein Emission in Heliotron J

K. Nagasaki[1], Y. Kato[2], Y. Oka[2], H. Igami[3], T. Minami[1], S. Kado[1], S. Kobayashi[1], S. Ohshima[1], Y. Nakamura, A. Ishizawa, T. Mizuuchi[1], H. Okada[1], S. Konoshima[1], R. Matoike[2], A. Iwata[2], M. Luo[2], P. Zhang[2], C. Wang[2], Y. Kondo[2], N. Marushchenko[4]

[1] Institute of Advanced Energy, Kyoto University, Uji, Kyoto, Japan
[2] Graduate School of Energy Science, Kyoto University, Uji, Kyoto, Japan
[3] National Institute for Fusion Science, Toki, Gifu, Japan
4 Max-Planck-Institut für Plasmaphysik, EURATOM Association, Greifswald, Germany

1. Introduction

Electron cyclotron emission such as Ordinary (O) and eXtraordinary (X) modes are used for electron temperature diagnostic in magnetic fusion devices. Since the ECE diagnostic is difficult to use above so-called cut-off density, use of electron Bernstein wave (EBW), an electrostatic wave propagating in hot magnetized plasmas, is proposed at the density where the O- and X-modes are not accessible. The EBWs have advantage of no density limit and high optical thickness even at low electron temperatures (~10eV). These aspects, along with high localization of their emission, makes EBWs suitable for electron heating and diagnostic of electron temperature profiles and the pitch angle of magnetic field at overdense plasmas, particularly in helical devices where high-density plasmas are available [1][2]. The issue is that since they cannot be measured directly due to the nature of electrostatic waves, they should be measured in the form of electromagnetic waves via mode conversion. In the case of EBW-slow X-mode-O-mode (B-X-O), which is one of the mode conversions, EBWs emitted from the resonance layer are converted to a slow X-mode at the upper hybrid resonance, and further converted to O-mode at the cut-off layer, and then propagating toward the outside of the plasma. In this paper, we show recent progress on experimental and theoretical study on electron temperature measurement with EBE radiation in the Heliotron J helical device.

2. Measurement of Electron Temperature Profile in Heliotron J

We have measured electron Bernstein emission (EBE) radiation with a multi-channel radiometer in the Heliotron J helical device. Heliotron J is a medium-sized stellarator/heliotron device [3][4]. The main device parameters are the plasma major radius $R = 1.2$ m, the averaged minor radius $a = 0.1$–0.2 m, the rotational transform $\iota/2\pi = 0.3$–0.8, and the maximum magnetic field strength on magnetic axis, B = 1.5 T.

The EBE diagnostic system consists of a heterodyne radiometer, a steerable antenna, and a waveguide transmission line [5]. The 16-channel heterodyne radiometer covers the frequency of 26-42 GHz, corresponding to the cut-off density of 0.86-2.25×10^{19} m^{-3}, which is conventionally produced in the Heliotron J device. The launcher and transmission line of

corrugated waveguides for the existing 70GHz ECRH/ECCD system is applied for the EBE diagnostic. The steerable antenna mirror can be scanned toroidally and poloidally to find the optimal angle for O-X mode conversion. Figure 1 shows a typical NBI discharge for the EBE diagnostic. A seed plasma is produced by a 2.45GHz microwaves without high power ECH. The ECE signal of both the fundamental O-mode and the second harmonic X-mode start increase as the electron density ramps up. When the density reaches a cut-off, the O-X window opens, and the fundamental O-mode ECE signal

Fig. 1. Time history of overdense plasma in Heliotron J. The ECE signals of fundament O-mode and second harmonic X-mode are plotted.

increases, while the second harmonic X-mode is kept low. As shown in Fig. 2, the fundamental ECE intensity depends on the viewing angle. The intensity is highest when both the toroidal and poloidal angles are -10 deg, which agrees with a ray tracing calculation result using the TRAVIS code [5]. The finite ECE signal is observed even far from the O-X window probably because of multi-reflected ECE radiation.
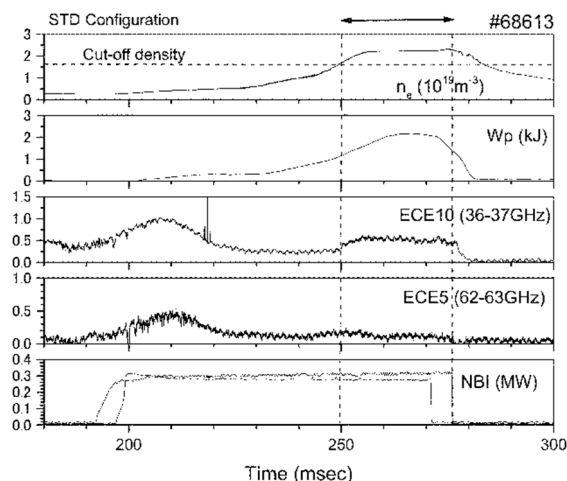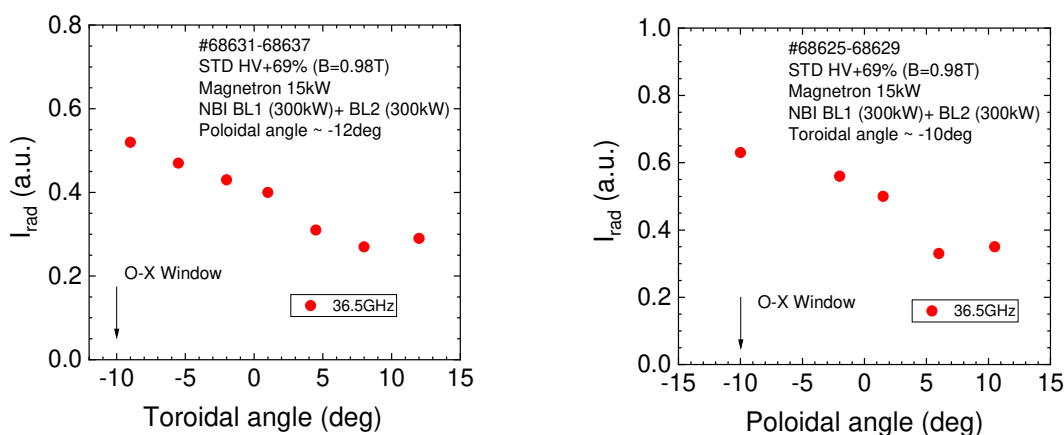
Fig. 2. Dependence of fundamental O-mode intensity on (a) toroidal angle and (b) poloidal angle. The O-X mode conversion window calculated by the TRAVIS code is -10 deg for both toroidal and poloidal angles.

The ECE radiation spectrum is expected to reflect T_e profile. Figure 3 shows an ECE radiation spectrum in overdense plasmas, which is estimated by subtracting the multi-reflection ECE signals. The signal intensity is relatively calculated with a noise source. The ECE frequency of the radiation peak is upshifted from the on-axis EC frequency. This may be due to the Doppler-shifted resonance of EBE with high $N_{\parallel}$. The frequency shift is estimated 1.6 GHz if we assume $T_e = 200$ eV and $N_{\parallel} = 2$. As shown in Fig. 4, the peak frequency is higher with an increase in the magnetic field. Determination of the radial radiation position requires a ray tracing calculation with the measured density profile. This is left for a future work.
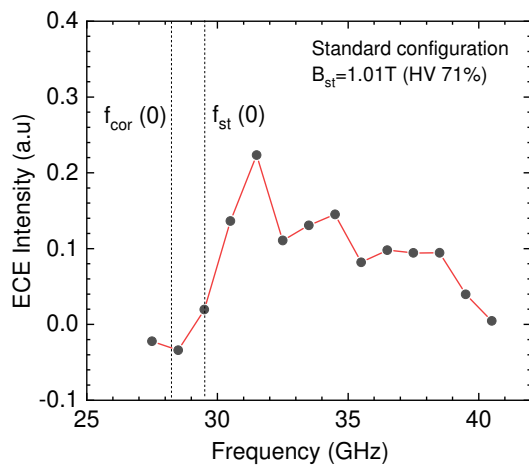
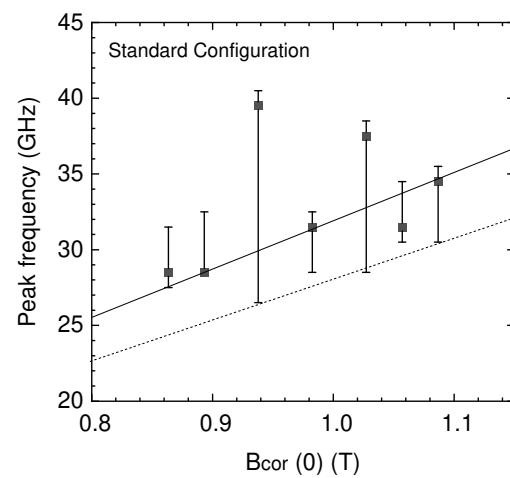Fig. 3. ECE radiation spectrum at overdense plasma of $n_e = 2 \times 10^{19}$ m^{-3}.

Fig. 4. Dependence of peak frequency on magnetic field at overdense plasmas of $n_e = 2 \times 10^{19}$ m^{-3}. The solid and dotted lines denote the fitting line and the fundamental EC frequency.

3. Simulation of O-X Conversion Using Finite Element Method

We have simulated the propagation of EC waves around the O-mode cut-off layer in a slab geometry with the simulation code, COMSOL Multiphysics® RF module. The wave frequency is $f = 42$ GHz, the uniform magnetic field is applied in the y direction, and the parabolic density profile has a gradient in the x direction. The Gaussian beam with the O-mode is launched toward the cut-off layer. The polarization of the injected wave is adjusted for full O-mode injection according to the injection angle. Figure 5 shows the beam propagation at several injection angles. It can be seen that some of the O-mode power is converted into the slow X-mode when the injection angle is close to the O-X window angle (Fig. 5(b)). The O-mode is refracted without mode conversion around the cut-off layer without any mode conversion.
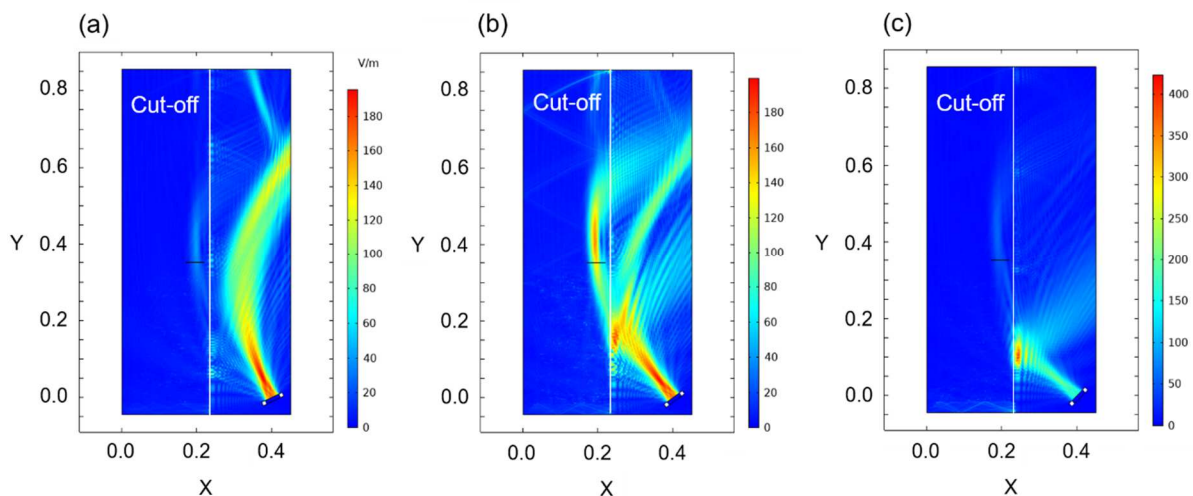

Fig. 5. Full wave beam propagation around O-mode cut off. The injection angles to the magnetic field are (a) 25 deg, (b) 36 deg and (c) 45 deg.

The beam parameters have been scanned to find out the maximal mode conversion efficiency. Figure 6 shows the dependence of the mode conversion efficiency on the Gaussian beam parameters at the optimal injection angle. The maximal mode conversion efficiency is obtained at 35.8 deg, which agrees with the optimal angle at the O-mode cut-off. The full wave beam propagation agrees with a conventional ray tracing calculation as shown in Fig. 7.
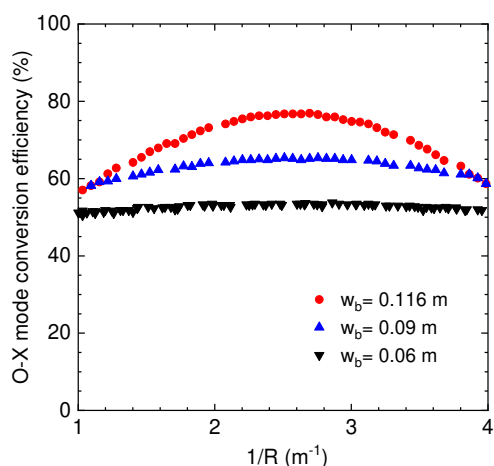

Fig. 6. Dependence of O-X mode conversion efficiency on beam curvature and beam size.
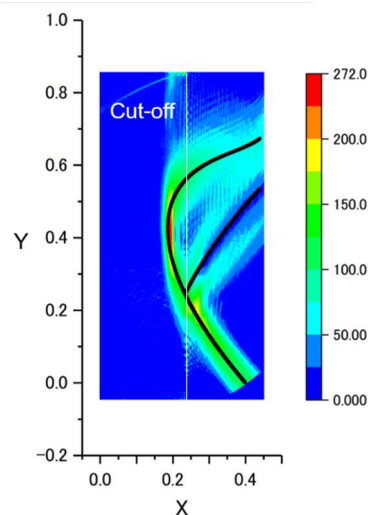

Fig. 7. Full wave beam propagation and ray tracing at optimum injection.

4. Summary

The EBE radiation via B-X-O mode conversion process has been studied for T_e measurement at overdense plasmas in the Heliotron J device. The finite ECE signals are observed when n_e exceeds the cut-off density, and the signal intensity is maximal when the antenna views the O-X mode conversion window, indicating that the EBE radiation is successfully measured. The ECE spectrum is Doppler-shifted due to high $N_\parallel$. The 2-D model calculation using the finite element method simulates the O-X mode conversion at the cut-off layer. The mode conversion efficiency is sensitive to the injection angle, the beam size and the beam waist position. The simulation results agree with the conventional ray tracing calculation. Estimation of T_e profile from the ECE spectra is underway.

Acknowledgments

References

[1]. H. Laqua, Plasma Phys. Control. Fusion 49 (2007) R1

[2]. K. Nagasaki and N. Yanagi, Plasma Phys. Control. Fusion 44 (2002) 409-422

[3]. M. Wakatani, et al., Nucl. Fusion, 40 (2000) 569

[4]. T. Obiki, et al., Plasma Phys. Control. Fusion 42 (2000) 1151

[5]. K. Nagasaki, et al., Plasma Fus. Res., 11 (2016) 2402095